IOP Publishing Semiconductor Science and Technology
Semicond. Sci. Technol. **34** (2019) 065019 (9pp) https://doi.org/10.1088/1361-6641/ab1d20

On the importance of the junction temperature on obtaining the charge transport parameters of a solar cell

J Mimila-Arroyo

Centro de Investigación y de Estudios Avanzados del Instituto Politécnico Nacional, Dpto. de Ing. Eléctrica-SEES, Av. Instituto Politécnico Nacional No 2508, México D.F. CP 07360, México

E-mail: jmimila@cinvestav.mx

Received 23 January 2019, revised 12 April 2019
Accepted for publication 26 April 2019
Published 22 May 2019

Abstract

The charge transport parameters (CTP) of a solar cell are extremely important as they provide the information required to do the fine tuning of its design and associated technology. This work demonstrates the necessity of knowing the junction temperature to extract them, other way their values might be wrong, misleading the device improvement efforts. Here the junction temperature and the CTP are extracted utilizing a dedicated structure similar to a bipolar junction transistor which allows to screen and separate the recombination current in the space charge region of the solar cell junction from that due to the injection-diffusion-recombination of minority carriers in its quasi-neutral regions. The additional pn junction is located beneath that of the solar cell, in such a way that the minority carriers injected into its base are able to reach the additional junction. Biasing the solar cell junction without biasing the additional one the neat separation of those currents is achieved. From the diffusion current reaching the additional junction the cell temperature is extracted as well as its diffusion saturation current. Then, with these two parameters the remaining ones are straightly obtained. Moreover, the current separation allows the cross verification of the extracted parameters. Additionally, the involved theory, model of Shockley, allows an estimation of the diffusion length and life time of the minority carriers in the solar cell base region. The method, applied to the n-GaInP/p-GaAs heterojunction solar cell shows that under the measurement conditions the true junction temperature was $T_0 = 296.343$ K, the studied structure at this temperature has a diffusion saturation current of $J_{0D} = 3.9 \times 10^{-19}$ A cm^{-2} and a recombination current density of $J_{0R} = 1.9 \times 10^{-12}$ A cm^{-2}, diffusion length and life time of minority carriers in the base region of $L_n = 0.46$ μm and $\tau_n = 1.2 \times 10^{-10}$ s, respectively. These saturation current values compared with those obtained through the conventional mathematical fit are orders of magnitude different.

Keywords: charge transport, solar cell, temperature

(Some figures may appear in colour only in the online journal)

1. Introduction

Improving the performance of solar cells, or any other semiconducting device, makes the knowledge of its charge transport parameters and their dependence on the physical properties of the active materials absolutely necessary. They provide relevant information on the device structure physical functioning as well as on its active materials performance, constituting a valuable feedback to improve its design and technological processing [1–4]. Notwithstanding, the literature reports containing outstanding results about solar cells performance, most of them, unhappily, containing no information about the charge transport properties of the corresponding devices, even if it is well known that they provide key

information about the physics involved in the structure and its materials behavior, as interfaces, free surfaces, etc. [5–13]. Moreover, sometimes it is attempted to provide one of the most important of those parameters; the dark saturation current of a solar cell junction, although often extracted in a too simple way and assuming non properly measured junction temperatures leading to erroneous results that will misguide the development efforts [2, 14–21]. In this work is proposed a reliable method to extract the functioning temperature and the charge transport parameters of a pn junction solar cell. It is based in the use of a properly designed structure involving an additional pn junction; "auxiliary junction' (AUJ) whose plane is parallel to that of the solar cell itself, placed in such a way that charge can be transferred from the solar cell junction into the auxiliary one. This structure actually approaches that of a bipolar junction transistor. The here proposed method has been applied to an n-InGaP/p-GaAs solar cell, forming the auxiliary pn junction with an additional n-GaAs layer beneath the p-GaAs of the solar cell. Our results show that the solar cell diffusion saturation current values obtained by the method here proposed and the conventional one, mathematical fit, can be orders of magnitude different. Moreover, this method provides additional information about the recombination current in the cell junction space charge region, in the quasi-neutral region of the base material and on the minority carriers diffusion length and life time in the solar cell base, physical information that cannot be obtained through the usual mathematical fit.

2. Theory

2.1. The isolated PN junction

Let us briefly review the charge transport properties of a pn junction (PNJ) solar cell in which the emitter, top active layer, is n-type and the base is p-type. According to the model of Shockley when the solar cell pn junction, at temperature T, is forward biased with a voltage V the current density that results; $J_{SC}(V,T)$, assuming no parasitic resistances, is due to two different mechanisms; the one due to the injection-diffusion-recombination of minority carriers into the quasi-neutral regions at each side of the PNJ space charge region and the second due to the electron-hole recombination in the depletion region of the solar cell junction, $J_D(V,T)$ and $J_R(V,T)$, first and second term of the right hand of equation (1), respectively.

$$J_{SC}(V,T) = J_D(V,T) + J_R(V,T) \tag{1}$$

According to Shockley model, such currents as functions of the applied bias and the junction temperature; V and T, are given by equation (2)

$$J_{SC}(V,T) = J_{0D}(T)\left[e^{\left(\frac{qV}{\eta_1 kT}\right)} - 1\right] + J_{0R}(T)\left[e^{\left(\frac{qV}{\eta_2 kT}\right)} - 1\right] \tag{2}$$

where J_{0D} and J_{0R} are the so-called saturation currents of the diffusion and pure recombination mechanisms, q is the electron charge, k the constant of Boltzmann, T the temperature, η_1 and η_2 are the ideality factors for the first and the second mechanisms, which according to Shockley's model are equal to 1 and 2 respectively. It is highlighted that J_{0D} and J_{0R} are exponentially dependent on the junction temperature although not with the same exponential dependence [22, 23].

In equation (1) $J_D(V,T)$ itself has two components; one resulting from electrons injected from the n-type emitter into the p-type quasi-neutral base region; $J_{Dn}(V,T)$, and the other due to holes injected from the p-type base into the emitter n-type neutral region; $J_{Dp}(V,T)$. Resulting, then, for each type of carrier a corresponding saturation current; $J_{0Dn}(T)$ and $J_{0Dp}(T)$. The total diffusion saturation current for the pn junction of the solar cell is given by

$$J_{0D}(V,T) = J_{0Dn}(T) + J_{0Dp}(T) \tag{3}$$

Both, electrons and holes, once injected into the base and emitter regions, respectively, become minority carriers that by the solely mechanism of thermal diffusion spread throughout their entire respective region simultaneously recombining. The minority carriers can reach the surfaces delimiting their respective region where they recombine with a rate proper to each surface. Considering a solar cell structure with finite n and p-type regions of lengths; d_n, and d_p respectively, such that when injected the minority carriers can reach the corresponding ending surfaces, the saturation currents for electrons and holes are given by equations (4) and (5) respectively [24].

$$J_{0Dn} = q\frac{n_{pi}^2(T)}{p_{po}}\sqrt{\frac{D_n}{\tau_n}} \times \left[\frac{\frac{S_n L_n}{D_n}Cosh\left(\frac{d_p - x_{0p}}{L_n}\right) + Sinh\left(\frac{d_p - x_{0p}}{L_n}\right)}{\frac{S_n L_n}{D_n}Sinh\left(\frac{d_p - x_{0p}}{L_n}\right) + \cosh\left(\frac{d_p - x_{0p}}{L_n}\right)}\right] \tag{4}$$

and

$$J_{0Dp} = q\frac{n_{ni}^2(T)}{n_{n0}}\sqrt{\frac{D_p}{\tau_p}} \times \left[\frac{\frac{S_p L_p}{D_p}Cosh\left(\frac{d_n - x_{0n}}{L_p}\right) + Sinh\left(\frac{d_n - x_{0n}}{L_p}\right)}{\frac{S_p L_p}{D_p}Sinh\left(\frac{d_n - x_{0n}}{L_p}\right) + \cosh\left(\frac{d_n - x_{0n}}{L_p}\right)}\right] \tag{5}$$

where n_{ni}, n_{pi}, n_{n0} and p_{p0} are the intrinsic carrier, the electron and the hole concentrations in the n-type and p-type regions respectively, D_p, D_n, τ_p, τ_n, L_p, L_n, S_p and S_n are the diffusion coefficients, lifetimes, diffusion lengths and surface recombination velocity of the minority carriers; holes and electrons, respectively, x_{on}, and x_{op} are the length of the depletion in the n and p region respectively. In these two equations, n_{ni}^2 and n_{pi}^2 are exponentially dependent with the temperature and the bandgap, Eg of the corresponding semiconducting material, i.e., they both are proportional to $\exp(-Eg/kT)$, and although D_n, D_p, L_n and L_p are also dependent on the temperature, this dependence is quite light compared with the exponential one, then in the sake of simplicity such dependence has not been

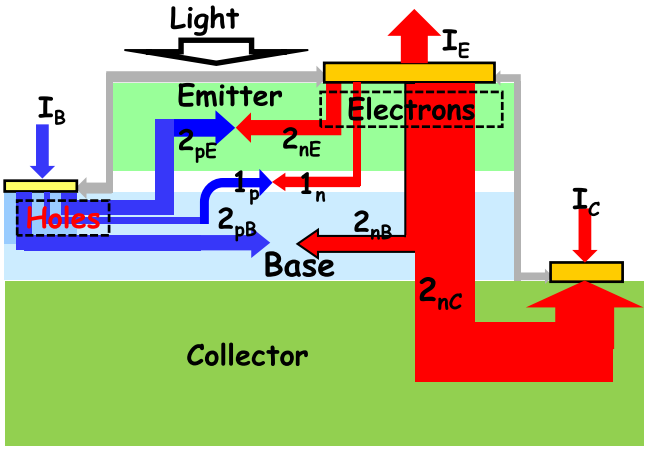

Figure 1. Schematics of the structure utilized in this method and the currents through it under the bias conditions; $V_{SC} > 0$ and $V_{BC} = 0$. In the emitter-base space charge the pure recombination current; arrows 1n and 1p. Currents J_{Dn} and J_{Dp}, equation (3), arrows 2_{nB} and 2_{pB} meeting in the middle of the neutral base region and arrows 2_{nE} and 2_{pE} meeting in the middle of the emitter region. Transferred current, arrow 2_{nC}. For the isolated solar cell in this structure, top junction between the emitter and the base, the collector ohmic contact is open and the auxiliary current schematized by the arrow 2_{nC} does not exist.

indicated. However once a value for J_{0D} (T) is obtained, it involves, of course, ell those factors.

The recombination current at the junction depletion region, last term of equation (2), results from the fact that the forward bias increases the electrons and holes concentrations in that region highly above their equilibrium values, triggering the electron-hole recombination process which takes place through energy levels around mid-gap. The saturation current of this mechanism is given by [22]

$$J_{0R}(V, T) = \frac{1}{2} q \sigma \nu_{th} N_T n_i W_0 \tag{6}$$

where, N_T is the recombination center concentration at the emitter-base space charge region, σ its capture cross section, v_{th}, the carriers thermal velocity and n_i, the intrinsic carrier concentration of the semiconductor where the recombination is taking place and W_0 ($=x_{0n} + x_{0p}$) is the junction depletion region width. Figure 1 schematizes the currents through the solar cell junction when forward biased. In that figure the solar cell junction (emitter-base) space charge recombination current corresponds to arrows 1n and 1p meeting in the middle of that region (white in the figure). Currents J_{Dn} and J_{Dp}, of equation (3), are shown by arrows 2_{nB} and 2_{pB} meeting in the middle of the neutral base region and arrows 2_{nE} and 2_{pE} meeting in the middle of the neutral emitter region, respectively. In this figure the auxiliary current 2_{nC}, that will be explained below, does not exists for the isolated solar cell of this structure, i.e., when the collector ohmic contact is kept open.

2.2. The bipolar junction transistor currents

As the proposed structure, actually corresponds to a bipolar junction transistor, let us briefly review, as well, the model of Shockley for its charge transport properties. In this structure when the solar cell junction is forward biased with voltage V all the currents already discussed for the pn junction of the solar cell appear through it. However, if the thickness of the p-type base neutral region is comparable to the electrons diffusion length; L_n, the current J_{Dn} splits in two components as well; J_{BDn} and J_{AU}. The first one is due to the recombination of electrons in the neutral region of the base (arrow 2_{nB}. in figure 1) and the second one to electrons that by the solely mechanism of thermal diffusion cross the neutral base region and reach the second junction (AUJ) whose permanent electric field transfers them into the n-type region of this auxiliary junction, i.e., the collector (arrow 2_{nC} in figure 1). Such current leaves the structure through the ohmic contact to the collector layer. Clearly, if this contact is left open this current does not exists. Through the ohmic contact to the base material leave the currents: J_{DBn}, (arrows 2_{nB} and2_{pB} in figure 1) plus J_{Dp} (arrows 2_{nE} and 2_{pE} in figure 1) plus the recombination current in the emitter-base space charge region, constituting all of them the base current, i.e., $J_B(V, T) = J_{Dp}(V, T) + J_{BDn}(V, T) + J_R(V, T)$. The ohmic contact to the emitter handles the solar cell current $J_E(V, T) = J_B(V, T) + J_{AU}(V, T)$ which corresponds to the solar cell current of equation (2). According to the model of Shockley and considering a forward bias applied only to the solar cell junction, $V > 3\,kT$ and, as said, no bias applied to the auxiliary junction, i.e., $V_{AU} = 0$, neither any parasitic resistances, the transferred current to the auxiliary junction and the base currents; $J_{AU}(V, V_{AU} = 0, T)$ and $J_B(V, V_{AU} = 0, T)$, are given by equations (7) and (8) respectively [22]

$$J_{AU}(V, V_{AU} = 0, T) = \frac{q D_n n_{pi}^2(T)}{p_{po} L_n Sinh\left(\frac{d_p - x_{0p}}{L_n}\right)} e^{\left(\frac{qV}{kT}\right)} = J_{0AU}(T) e^{\left(\frac{qV}{kT}\right)} \tag{7}$$

And

$$J_B(V, V_{AU} = 0, T) = \left\{ J_{ODp}(T) + \frac{q D_n n_{pi}^2(T)\left[Cosh\left(\frac{d_p - x_{0p}}{L_n}\right) - 1\right]}{p_{p0} L_n Sinh\left(\frac{d_p - x_{0p}}{L_n}\right)} \right\} e^{\frac{qV}{kT}} + J_{0R}(T) e^{\frac{qV}{2kT}} = [J_{ODp}(T) + J_{ODBn}(T)] e^{\frac{qV}{kT}} + J_{0R}(T) e^{\frac{qV}{2kT}} \tag{8}$$

where J_{0Dp} corresponds to equation (5), the saturation current due to the holes injected into the solar cell emitter and the second term in the brackets of equation (8) to J_{0DBn}, the saturation current due to the electrons injected into the p-type solar cell base that do not reach the auxiliary junction and recombine there. Here the ideality factors for the diffusion and recombination mechanisms are considered those proposed by Shockley; 1 and 2, respectively. In the sake of simplicity equation (8) can be rewritten as

$$J_B(V, T) = J_{0EBD}(T) e^{\frac{qV}{kT}} + J_{0R}(T) e^{\frac{qV}{2kT}} \tag{9}$$

where J_{0EBD} represents $J_{0Dp}(T) + J_{ODBn}(T)$, i.e., the currents

due to the injection-diffusion-recombination mechanism. From equations (7) and (8), $J_{ODBn}(T)$ is obtained as a function of $J_{OAU}(T)$,

$$J_{0DBn}(V, T) = J_{0AU}(T)\left[Cosh\left(\frac{d_p - x_{0p}}{L_n}\right) - 1\right] \quad (10)$$

It should be stressed that the two pre-exponential terms related to the injection-diffusion-recombination mechanism in the brackets of equation (8), normally are of different magnitude. That being true for absolutely any pn junction, that is to say that one of those terms will dominate the base diffusion current. Then, the solar cell current for forward bias >3 kT and no series nor parallel parasitic resistances is given by

$$\begin{aligned} J_{SC}(V, T) &= J_{AU}(V,\ V_{AU} = 0, T) + J_B(V, V_{AU} = 0, T) \\ &= [(J_{0AU}(T) + J_{0Dp}(T) + J_{0DBn}(T)]e^{\left(\frac{qV}{kT}\right)} \\ &++\ J_{0R}(T)e^{\left(\frac{qV}{2kT}\right)} = J_{0D}(T)]e^{\left(\frac{qV}{kT}\right)} + J_{0R}(T)e^{\left(\frac{qV}{2kT}\right)} \end{aligned} \quad (11)$$

Which corresponds to equation (2). Finally, the method here presented uses the ratio of the current given by equation (7) to that given by equation (9), which corresponds to the so-called transistor current gain and is given by

$$\beta(V, T) = \frac{J_{OAU}(T)e^{\left(\frac{qV}{kT}\right)}}{J_{OEBD}(T)e^{\frac{qV}{kT}} + J_{OR}(T)e^{\frac{qV}{2kT}}} \quad (12)$$

3. Experimental

3.1. Sample preparation and measurements

The structure to extract the charge transport parameters of the solar cell was constructed as follows. To obtain the proposed additional junction first an n-type Si doped GaAs layer was grown on the conducting n-GaAs substrate, then the solar cell base, p-type carbon doped GaAs, simultaneously forming the auxiliary junction and the base of the solar cell. Finally the n-GaInP emitter was grown, forming the hetero/junction solar cell. Each of these layers was provided with its own ohmic contact, as shown in figure 1. The n-GaInP layer having an electron concentration around 10^{18} e-cm^{-3} and the p-GaAs was 100 nm thick with a hole concentration close to 10^{20} holes-cm^{-3} displaying a hole mobility of 70 cm^2- V^{-1} s^{-1}. All the results presented below were obtained on a solar cell displaying this structure. The area of the solar cell was $100 \times 100\ \mu m^2$. The structure was grown by MOCVD, mesas were done using wet etching and contacts by vacuum evaporated metallic alloys and rapid thermal anneal to reach ohmicity. Measurements were done using an HP4145 Semiconductor Parameter Analyzer. The auxiliary junction maintained at zero bias when the current through it was measured and when measuring the solar cell alone the contact on the n-GaAs layer of the auxiliary junction was kept open. The temperature of the stage where the solar cell was placed for measurements was determined utilizing a Pt calibrated

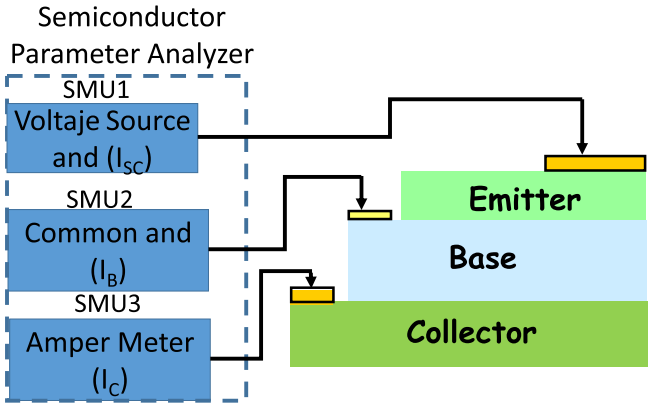

Figure 2. Schematics of the measurement set up; first SMU (Source Measurement Unit) is connected to the base constituting the common and simultaneously measuring the base current, second SMU is connected to the emitter providing the bias and simultaneously measuring the $J_{SC}(V_{SC}, T)$ current and third SMU connected to the collector to measure the $J_{AU}(V_{SC}, T)$ current.

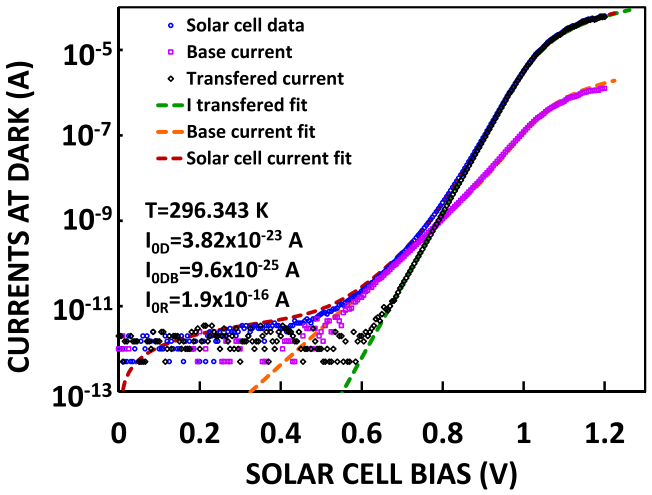

Figure 3. Currents at dark through the n-InGaP/p-GaAs/n-GaN solar cell structure, as a function of V_{SC}, the bias applied to the n-InGaP/p-GaAs junction, keeping the auxiliary junction; p-GaAs/n-GaAs beneath the solar cell at zero bias; solar cell current, $J_{SC}(V_{SC}, T)$, empty blue circles, base current, $J_B(V_{SC}, T)$, fuchsia empty squares and transferred current $J_{AU}(V_{SC}, T)$, empty black diamonds, respectively. Green dotted line fit to the transferred current, Orange dotted line fit to the base current, in the sake of clarity without considering a parasitic parallel resistance and brown dotted line fit to the solar cell current.

resistance. However, considering that this temperature might be different from that of the solar cell junction, the last one will be referred as T_x. The current voltage data to be presented and discussed below were obtained according to the scheme shown in figure 2.

Figure 3 shows a typical plot, at dark, of the three currents through the solar cell structure versus the forward bias of the cell junction, i.e., the bias is applied between the tope n-GaInP layer and the p-GaAs and the currents measured being $I_{SC}(V,T)$, $I_B(V,T)$ and $I_{AU}(V,T)$, through the ohmic contacts on the GaInP, p-GaAs and lower n-GaAs layers, empty blue circles, fuchsia empty squares and empty black diamonds, respectively. It is highlighted that the only bias

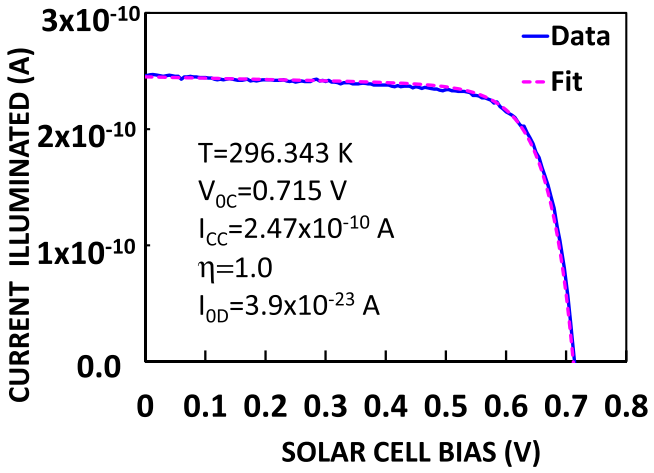

Figure 4. Current-voltage curve of the 100 × 100 μm^2 n-InGaP/p-GaAs solar cell under illumination, at 'room temperature', collector contact left open.

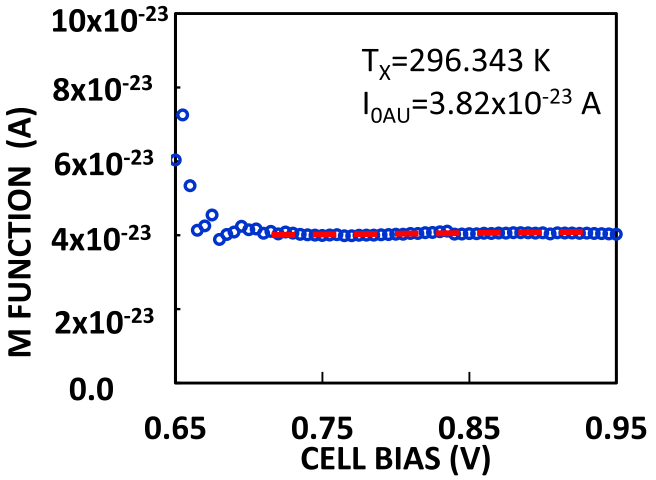

Figure 5. Plot of $M(J_{AU},V_{SC}, T_x, T_0) = J_{AU}(V_{SC}, T_x)\exp(-qV_{SC} / kT_0)$ as a function of V_{SC} with already substituted in it the value of $T_0 = 296.343$ K that yields M = cte = $J_{0AU}(296.343)$.

applied to the structure is to the solar cell junction. Although this structure was designed to study the charge transport properties and not the solar cell performance, figure 4 displays its current voltage characteristics under week illumination. The stage measured temperature was 300.5 K. Extracting the charge transport parameters means, at least, obtaining the values for J_{0D}, J_{0R}, η_1 and η_2 of equation (2) that fit the best the experimental data of figure 3.

3.2. Temperature and charge transport parameters extraction

The very first thing to be remarked in figure 3 is the fact that $I_{SC}(V, T)$ data seem to follow an exponential behavior for currents between 10^{-8}–10^{-6} A. However, a close careful inspection shows that this is not the case at all, as those data (empty blue circles) when compared with the ones displaying, according to equation (7), a true exponential behavior, those corresponding to I_{AU} (V, $V_{AU} = 0$, T) black empty diamonds, is easily concluded that $I_{SC}(V, T)$ data are not on a straight line and this even in the region where their behavior seems to be the most linear in that semi-log plot. By another way, it should be kept in mind that the transferred current into the auxiliary junction, I_{AU}, is due only to electrons injected from the solar cell n-InGaP top layer into the base, which solely by thermal diffusion reach the auxiliary junction and being transferred into the collector. As there is no bias applied to the collector-base junction ($V_{CB} = 0$ V), this transferred current is totally free of any parasitic contribution and thus strictly following, the model of Shockley. As clearly seen in figure 3, where the transferred current, empty black diamonds, follows an exponential behavior at least through six decades, only deviating from it for currents higher than 1 μA by the effect of parasitic series resistance. It is also seen that both currents; the emitter's and the transferred one, for values higher than 10 nA, are almost equal. This means that most of the injected electrons into the base reach the auxiliary junction which is verified by the small current measured through the base contact for that same current interval. To extract the charge transport parameters; J_{0D}, J_{0R}, η_1 and η_2 it is utilized a method comprising just two main steps. First, the true temperature of the solar cell junction is obtained and the transferred saturation current; T_x and J_{0AU}, respectively. Then, with these parameters the diffusion saturation current in the base which complements the solar cell saturation diffusion current, and the recombination in the cell space charge region; J_{0EBD} and J_{0R}, are obtained.

The solar cell junction temperature is extracted with a new and highly reliable method, utilizing the experimental data of $I_{AU}(V, T_x)$ in the function $M(I_{AU},V, T_x, T_0) = I_{AU}(V, T_x)\exp(-qV/kT_0)$, where T_x is the unknown solar cell junction temperature at the measurement time and T_0 is a parameter having units of temperature that allows to obtain T_x, the true junction temperature. Substituting $I_{AU}(V, V_{AU} = 0, T_x)$ from equation (7) into the M function, results in $M(V, T_x, T_0) = I_{0AU}(T_x)\exp[qV(1/kT_x\text{-}1/kT_0)]$. Clearly, there is a value for the unknown parameter T_0 for which the function $M(V_{SC}, T_x, T_0)$ becomes a constant equal to $J_{0AU}(T_x)$. This occurs when to the unknown T_0 parameter is given a value that results to be equal to T_x, the searched junction temperature [24–26]. It is highlighted that the above procedure does not constitutes a fit but rather a rigorous mathematical procedure based on the model of Shockley for the transistor currents. Figure 5 shows the plot of the M function obtained utilizing the $I_{AU}(V)$ data of figure 3, with $T_0 = 296.343$ K, value that yields $M(V, T_x, T_0)$ a constant. The $T_0 = 296.343$ K corresponds to the true temperature of the junction cell and the value of J_{0AU} at this temperature results to be; $J_{0AU}(T_x = 296.343\text{ K}) = 3.82 \times 10^{-19}\text{ A/cm}^{-2}$. The temperature difference between that of the measure stage and that of the cell junction, although just 3%, is quite important, as it will be shown later. Using these two extracted parameters in equation (7) and a proper value for the parasitic series resistance (the method to extract it will be published elsewhere), the fit to the transferred current data $I_{AU}(V, 296.343\text{ K})$ is shown in figure 3, green dotted line, as seen it is

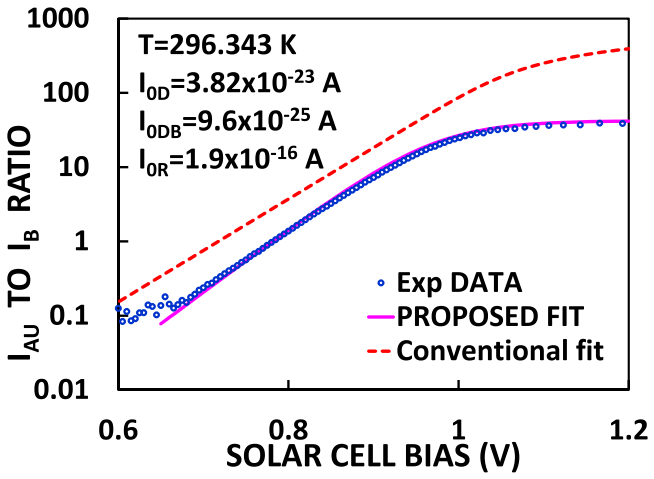

Figure 6. Plot of the ratio $J_{0AU}(V_{SC}, 296.343)/J_B(V_{SC}, 296.343)$, blue empty circles, the fit using equation (10) with the parameters given in this figure, fuchsia line going through the experimental data and the same ratio obtained using the charge transport parameters obtained through a conventional mathematical fit, red dotted line.

excellent over the entire data range of eight decades. The remaining injection-diffusion and pure recombination saturation currents, equation (9); J_{0EBD} ($T_x = 296.343$ K) and $J_{0R}(T_x = 296.343$ K), respectively, are not extracted by the mathematical fit of the corresponding data using equation (9) but through equation (12). Figure 6 shows the plot of the ratio of the transferred current data to those of the base current; $I_{AU}(V_{SC}, 296.343$ K$)/I_B(V_{SC}, 296.343$ K), empty blue circles. Then using the already extracted T_x and J_{0AU} values in equation (12) and considering J_{0R} zero, the current ratio results a constant equal $J_{0AU}(T)/J_{0EBD}(T)$, which corresponds to the data plateau of figure 6. The value for J_{0EBD} (T), is just J_{0AU} divided by the mean value of the current gain plateau, yielding; J_{0EBD} (T) $= 9.6 \times 10^{-21}$ A cm^{-2}. It is underlined that with the measurements done here is impossible to establish if this value corresponds to J_{0Dp} or J_{0DBn}. J_{0R} is obtained through the fit of the data in figure 6 corresponding to the roll-off of the current gain for lower biasing voltages, using equation (12), resulting $J_{0R} = 1.9 \times 10^{-12}$ A cm^{-2}. With just these two parameters and the junction temperature, of course, the excellent fits to the $I_B(V, T)$ data are obtained, orange line in figure 3, and to $J_B(V, T)/J_{AU}(V, T)$ ratio, data of figure 6 fuchsia line. For the fit of $I_B(V, T)$ the already mentioned series resistance has been considered. It should be highlighted that actually the fit of data of figure 6 constitutes, at the same time, a cross verification of the obtained values for all the above parameters, this will be more clear below at the discussion of these results. Finally J_{0D} $(=J_{0AU} + J_{0EBD}) = 3.9 \times 10^{-19}$ A cm^{-2}, substituting these parameters in equations (2) or (11) and considering the same series resistance already used for fitting $I_{AU}(V, 296.343$ K), the fit to the solar cell current of figure 3 data is obtained, red color dotted line, a parasitic parallel resistance $R_P \sim 10^{10}\,\Omega - \text{cm}^2$ has been considered. Additionally, using the value for J_{0EBD}, a minimum value for the electrons diffusion length in the base; L_n, can be established. As $J_{0DBn} = 9.6 \times 10^{-21}$ A cm^{-2}, utilizing equation (10) and assuming x_{0p} negligible, a value for $L_n = 0.46\,\mu$m is obtained. If the considered value of 9.6×10^{-21} A cm^{-2} does not correspond to J_{0DBn}, then that saturation current value corresponds J_{0Dp}, in this case L_n has to be higher than 0.46 μm. Moreover, using the base majority carrier concentration already given, an electron mobility of 700 cm^2-V^{-1}-s^{-1} can be assumed [22], leading to a minority carriers life time at the base of $\tau_n = 1.2 \times 10^{-10}$ s. A few millimeters away from the discussed structure there was another one identical, for which the corresponding values were, for $L_n = 0.56\,\mu$m and $\tau_n = 1.8 \times 10^{-10}$ s, yielding information about the homogeneity of the structure throughout the wafer. The above electron life time in the solar cell base agree with those reported in [27].

The above described procedure to extract the solar cell temperature and its CTP utilizing an alike bipolar junction transistor structure can be summarized in four steps; The experimental one measuring the three currents through the structure and three additional steps of simple and straightforward data processing: First, obtain the three currents polarizing only the solar cell junction while the auxiliary junction is kept at zero bias, i. e., $V > 0$ and $V_{BC} = 0$, measuring; $I_{SC}(V, V_{BC} = 0, T_x)$, $I_B(V, V_{BC} = 0, T_x)$ and $I_{AU}(V, V_{BC} = 0, T_x)$, as shown in schematics of figure 2. Second, extract the solar cell junction temperature and the pre-exponential term of $I_{AU}(V, V_{BC} = 0, T_x)$; T_x and J_{0AU}, respectively, utilizing the function $M(I_{AU},V, T_x, T_0) = I_{AU}(V, T_x)\exp(-qV/kT_0)$, proposing an arbitrary value for T_0. Then, T_0 has to be varied to find a value for which the M function results to be a constant. The T_0 value for which this condition is met is the real solar cell junction temperature and the corresponding value of the M function being J_{0AU} at that temperature. Third, extract the pre-exponential term I_{0EBD} (T_x), building up the function $\beta(V, T_x) = I_{AU}(V, T_x)/I_B(V, T_x)$, the constant value of this function for the high V values corresponds to the ratio $I_{0AU}(T_x)/I_{0EBD}(T_x)$, from which $J_{0EBD}(T_x)$ is straightforwardly obtained. To extract the pre-exponential term J_{0R} (T_x), the already found parameters; T_x, I_{0AU} (T_x) and $I_{0EDB}(T_x)$ are substituted into equation (12) and by fitting the far left data of figure 6, $I_{0R}(T_x)$ is obtained.

4. Discussion

The above extracted charge transport parameters allow an extremely good fit to the experimental data of the three measured currents the solar cell structure and the additional junction. As said, if these parameters are reliable provide valuable information for the improvement of the device by the fine tuning of its design and technology. Let us now compare our results with those obtained utilizing the measuring stage temperature and the usual procedures to extract them, of course, the same experimental data are considered, blue empty circles from figure 3.

As already said, very often the charge transport parameters are obtained in a too simple way considered that equation (13) rules the relation current-voltage of the cell and

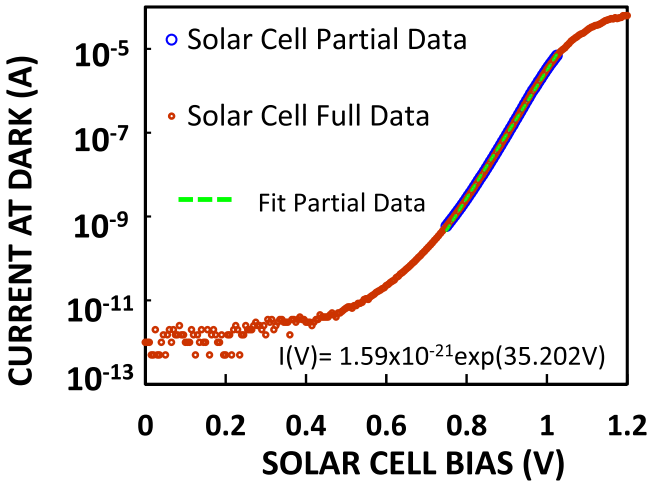

Figure 7. Experimental $J_{SC}(V_{SC}, T)$ data of figure 1 and part of them where the behavior seems to be linear in this semi-log presentation, blue empty circles, as well as the fit, green line, and the equation yielding the green line.

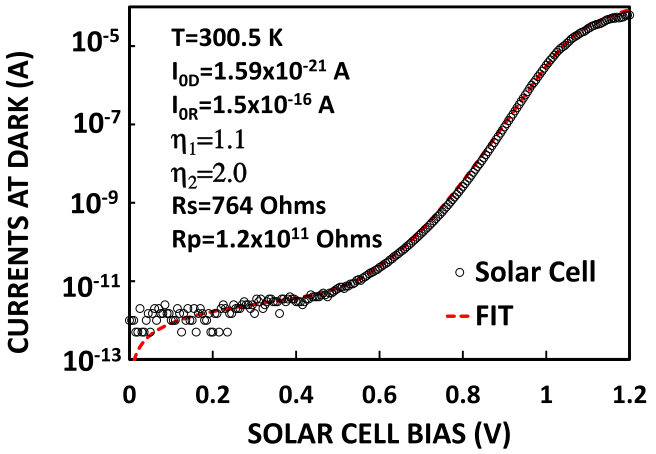

Figure 8. Experimental $J_{SC}(V_{SC}, T)$ data of figure 1 and their fit, orange dotted line, using the mathematical approach which yields completely different charge transport parameters from those obtained using the true junction temperature.

using it, the 'dark saturation' current is obtained; J_{0D}, which might be erroneous. For instance, in the case of the structure studied here, data plotted in figure 4, using the measured stage temperature (300.5 K) and $\eta_1 = 1.0$ in equation (13), it is obtained $J_{0D} = 2.7 \times 10^{-18}\,\mathrm{A\,cm^{-2}}$, value about one order of magnitude higher than the one obtained using the proper junction temperature and the here proposed method. That wrong value will provide erroneous information to the cell developer.

$$J_{SC}(V, T) = J_{0D}(T)[e^{\left(\frac{qV}{\eta_1 kT}\right)} - 1] - J_{CC}(T) \qquad (13)$$

On the other way if the extraction of the charge transport parameters is attempted just through a mathematical fit of the solar cell current data with equation (2), which is often done by first fitting their part that display an exponential behavior close to that due to the injection-diffusion-recombination mechanism. For instance, figure 7 shows the cell current experimental data from figure 3 (blue empty circles) twice, the full data, brown empty circles, and the partial set that allows a reasonable last squares fit to an exponential, blue big empty circles, as well as the fit to this last set of data, green dotted line. The equation that fits the best the blue partial data is $J(V) = 1.59 \times 10^{-17}\exp(35.202\,V)$, A/cm^2, normally the above pre-exponential term is associated with the diffusion saturation current of the junction cell. This is a very contrasting result as this value is more than 40 times bigger than the one obtained with the method here proposed with the true junction temperature and 7 times the value obtained with equation (13). Moreover, the factor of V in the exponent of the above equation; 35.202 $1/V$, corresponds to $1/(\eta_1 kT)$ in equation (2), considering that the ideality factor is 1.0, it results that the junction cell temperature has to be 329.6 K, value far away from the one measured for the stage where the solar cell is placed while measured. Clearly this value is unreasonable. On the other way, if the stage temperature is considered to be that of the cell junction, to fit the data, results necessary to introduce in the exponential factor in the first term of the right hand side of equation (2), a value for $\eta_1 = 1.1$, which is 10% higher than the obtained using the true junction temperature. To extract the second pre-exponential term of that equation, it might be considered $\eta_2 = 2$ and evidently the same junction temperature, obtaining $J_{0R} = 1.6 \times 10^{-12}$ A. With these four parameters the fit shown in figure 8 is obtained, red dotted line, this fit seems at least as good as the one shown in figure 3, brown dotted line. However, when these last charge transport parameters are used to fit the I_{AU} to I_B ratio of figure 6, the red dotted line is obtained, which is far away from the experimental data. Clearly the last CTP values just do not are able to comply the cross verification constituted by the data of figure 6. Thus, realizing the fit of current-voltage experimental data of solar cells, just as a mathematical procedure might lead to results that do not correspond to the real cell physical parameters nor the physical processes through the device, as do the method here proposed using the true solar cell junction temperature. The difference between these two values is due to two main factors. First, in the mathematical fit the diffusion saturation current is extracted from data containing all the components of the current through the cell junction resulting from its forward bias, that is to say, it contains spurious, recombination and injection diffusion currents (blue empty circles in figure 3), i.e., these data are contaminated by all of these currents which do not follow a pure exponential with a ideality factor of one. Forcefully the fit yields a value that is different from the one obtained through this new method as in it the utilized data are those containing only the injection-diffusion current (black empty diamonds in figure 3) that follow an exponential with an ideality factor of one.

5. Conclusions

We have demonstrated that the knowledge of the true solar cell junction temperature is mandatory to extract reliably its charge transport parameters. The method utilized to do that is

a new one which uses a dedicated structure similar to a bipolar junction transistor with the solar cell junction placed at its top. Such structure allows to extract the true junction temperature and screen and separate the cell recombination current in its junction space charge region from that due to the injection-diffusion-recombination of minority carriers in its quasi-neutral regions. Being that current separation which enables to extract the true junction temperature permitting to get reliable charge transport parameters, simultaneously providing information about the recombination in the neutral regions of the solar cell. All of this, applied to the n-GaInP/p-GaAs heterojunction solar cell allowed to demonstrate how important is to know the true junction temperature to extract the true charge transport parameters. Additionally, this method permits the cross verification of the extracted parameters and information about the diffusion length and life time of minority carriers and the recombination in the quasi-neutral region of the base region. And last but not least, it is demonstrated that the parameters obtained as a pure mathematical exercise might be unable to fit part of the data obtained with this dedicated structure and yield erroneous values that might misguide the development of a solar cell.

Acknowledgments

The author wishes to express his deepest gratitude to M en C R Huerta for valuable technical assistance.

ORCID iDs

J Mimila-Arroyo https://orcid.org/0000-0001-7622-1617

References

[1] Perl E E, Kuciauskas D, Simon J, Friedman D J and Steiner M A 2017 Identification of the limiting factors for high-temperature GaAs, GaInP, and AlGaInP solar cells from device and carrier lifetime analysis *J. Appl. Phys.* **122** 233102

[2] Kayes B M, Nie H, Twist R, Spruytte S G, Reinhardt F, Kizilyalli I C and Higashi G S 2011 27.6% Conversion effiency, a new record for single-junction solar cell under 1 sun illumination *Proc. of the 37th IEEE Photovoltaic Specialists Conf.* (https://doi.org/10.1109/PVSC.2011.6185831)

[3] Perl E E, Simon J, Geisz J F, Lee M L, Friedman D J and Steiner M A 2016 Measurements and modeling of III–V solar cells at high temperatures up to 400 °C *IEEE J. of Photovol.* **6** 1345–52

[4] Kobayashi E, Watabe Y, Hao R and Ravi T S 2015 High efficiency heterojunction solar cells on n-type kerfless mono crystalline silicon wafers by epitaxial growth *Appl. Phys. Lett.* **106** 223504

[5] Yoshikawa K, Kawasaki H, Yoshida W, Irie T, Konishi K, Najano K, Uto T, Adachi D, Kanematsu N and Yamamoto K 2017 Silicon heterojunction solar cell with interdigitated back contacts for a photoconversion efficiency over 26% *Nature Energy* **2** 17032

[6] Benick J *et al* High-efficiency n-type HP mc silicon solar cells *IEEE J. of Photovol.* **7** 2017 1171–5

[7] Venkatasubramanian R, O'Quinn B C, Hills J S, Sharps P R, Timmons M L, Hutchby J A, Field H, Ahrenkiel A and Keyes B 1996 18.2% (AM1.5) efficient GaAs solar cell on optical-grade polycrystalline Ge substrate *Proc. of the 25th IEEE PVSC (Washington)* pp 31–6

[8] Wanlass M 2017 Systems and methods for advanced ultra-high-performance InP solar cells *US Patent* 9,590,131 B2

[9] Kato T *et al* Enhanced efficiency of Cd-free Cu(In,Ga)$(Se,S)_2$ minimodule via (Zn,Mg)O second buffer layer and alkali post treatment *IEEE J. of Photovol.* **7** 2017 1773–80

[10] Jackson P, Hariskos D, Wuerz R, Kiowski O, Bauer A, Magorian T and Powalla M 2015 Properties of Cu(In,Ga) Se2 solar cell with new record efficiencies up to 21.7% *Phys. Stat. Soli. RSL* **9** 201409520

[11] Sun K, Yan C, Liu F, Huang J, Zhou F, Stride J A, Green M and Hao X 2016 Over 9% efficient kesterite Cu_2ZnSnS_4 solar cell: fabricated by using $Zn_{1-x}Cd_xS$ buffer layer *Adv. Energy Mater.* **6** 1600046

[12] Franklin E *et al* 2016 Design, fabrication and characterisation of a 24.4% efficient interdigitated back contact solar cell *Prog. Photovolt: Res. Appl.* **24** 411–27

[13] Feldmann F, Bivour M, Reichel C, Hermle M and Glunz S W 2014 Passivated rear contacts for high-efficiency n-type Si solar cells providing high interface passivation quality and excellent transport characteristics *Sol. Energy Mater. Sol. Cells* **120** 270–4

[14] Huang C Y, Lee W C and Lin A 2016 A flatter gallium profile for high-efficiency Cu(In,Ga)$(Se,S)_2$ solar cell and improved robustness against sulfur-gradient variation *J. of Appl. Phys.* **120** 094502

[15] Wang W, Winkler M T, Gunawan O, Gokmen T, Todorov T K, Zhu Y and Mitzi D B 2013 Device characteristics of CZTSSe thin-film solar cells with 12.6% effi ciency *AD. Energy Mat.* **4** 1301465

[16] Venkatasubramanian R, Timmons M L, Sharps P R and Hutchby J A 1997 15.8%-Efficient (1-SUN, AM 1.93) GaAs solar cell on optical grade polycrystalline Ge substrate *Proc. of the 23th IEEE PVSC (Washington)* 691–5

[17] Xiang X B, Du W H, Chang X L and Yuan H R 2001 The study on high effcient $Al_xGa_{1\sim x}As$/GaAs solar cells *Sol. Energy Mater. Sol. Cells* **68** 97–103

[18] Bär M, Bloeck U, Muffler H J, Lux-Steiner M C, Fischer C-H, Giersig M, Niesen T P and Karg F 2005 Cd^{2+}/NH_3-treatment of Cu(In,Ga)$(S,Se)_2$: impact on the properties of ZnO layers deposited by the ion layer gas reaction method *J. Appl. Phys.* **97** 014905

[19] Ramanathan K, Teeter G, Keane J C and Noufi R 2005 Properties of high-efficiency $CuInGaSe_2$ thin film solar cells *Thin Solid Films* **480–481** 499–502

[20] Repins I, Contreras M A, Egaas B, DeHart C, Scharf J, Perkins C L, To B and Noufi R 2008 19.9%-efficient ZnO/CdS/$CuInGaSe^2$ solar cell with 81.2% fill factor *Prog. Photovolt: Res. Appl.* **16** 235–9

[21] Jackson P, Hariskos D, Lotter E, Paetel S, Wuerz R, Menner R, Wischmann W and Powalla M 2011 New world record efficiency for Cu(In,Ga)Se2 thin-film solar cells beyond 20% *Prog. Photovolt: Res. Appl.* **19** 894–7

[22] Sze S M 1981 *Physics of Semiconductor Devices* 2nd edn (New York: Wiley)

[23] Kelvey J P M 1966 *Solid State and Semiconductor Physics* (Malabar, FL: R E Krieger)

[24] Mimila-Arroyo J 2013 Free electron gas primary thermometer: the bipolar junction transistor *Appl. Phys. Lett.* **103** 193509

[25] Mimila-Arroyo J 2016 Electrical determination of the bandgap energies of the emitter and base regions of bipolar junction transistors *Jour. of Appl. Phys.* **120** 164508

[26] Mimila-Arroyo J 2017 The free electron gas primary thermometer using an ordinary bipolar junction transistor approaches ppm accuracy *Rev. Sci. Instrum.* **88** 064901

[27] Tiwari S and Wright S L 1990 Material properties of p-type GaAs at large dopings *Appl. Phys. Lett.* **56** 563